Journal of Engineering Physics and Thermophysics, Vol. 80, No. 4, 2007

USE OF EQUATIONS FOR TRANSFER OF PARTICLE PULSATION CHARACTERISTICS FOR CALCULATING TWO-PHASE FLOWS IN THE STABILIZED SECTION OF A TUBE

B. B. Rokhman

UDC 532.529:662.62

A stationary isothermal system of equations defining the behavior of a two-phase rising flow in the region of steady motion of a gas suspension in an axially symmetric channel has been developed. The equation of motion of the carrying medium is closed using a one-parameter model of turbulence, and the equation of momentum transfer in the dispersed phase is closed with the use of the equations for the second, third, and fourth moments of the pulsation velocities of the particles. The main mechanisms of two-phase turbulent flows were numerically investigated.

It is difficult to experimentally investigate the mechanisms of mass and momentum transfer in two-phase turbulent flows consisting of a gas and particles; therefore, of great importance is construction of mathematical models for numerical investigations of such flows. To describe a gas-dispersion flow, it is necessary, first of all, to construct the initial system of actual mass- and momentum-transfer equations. In [1], a change from a mixture with a discrete structure to the motion of two continual media was done with the use of the statistical approach. By averaging the microequations over the space, the Euler equations of mass and momentum conservation were obtained for each phase. In [2], these equations were averaged over time by the Reynolds procedure. The system of equations obtained in this way was nonclosed because, in addition to the average values of the velocity, density, concentration, pressure, and other parameters, it included the second moments of the pulsation characteristics of the gas suspension. The moments defining the solid phase are usually calculated with the use of local-equilibrium models [2–4]. In these models, the turbulent shear stresses in the dispersed phase are expressed in terms of the Reynolds stresses in the carrying medium. The pulsation characteristics of the particles can also be determined from the gradient-type algebraic expressions constructed using the Boussinesq hypothesis for a one-phase turbulent flow. Since most of the gradient-type models are constructed in a purely phenomenological way on the basis of an analogy with the corresponding transfer characteristics of one-phase flows, they include a large number of empirical constants, which can lead to the appearance of significant errors in calculating the parameters of the dispersed phase. Along with the local-equilibrium algebraic models defining the turbulent momentum transfer in the dispersed phase, differential models including equations of transfer of the desired correlations are widely used [5–7]. These models allow one to describe the nonlocal effects of transfer of the dispersed-phase pulsation characteristics — the mechanisms of transfer of the turbulent momentum and the pseudoturbulent one (arising as a result of the interparticle collisions). In this approach, the differential equations for the second moments include the third moments. The Reynolds procedure allows one to construct the third-moment transfer equations that will include the fourth moments and so on. Therefore, to obtain a closed system of equations, it is necessary to terminate this process at any stage, i.e., to introduce additional hypotheses for the relations between the "higher" and "lower" correlations. In [6], the equations of second-moment transfer were closed using gradient representations, such as $\langle v'_p v'_p v'_p \rangle = -\eta_{t,p} \partial \langle v'_p v'_p \rangle / \partial r$). In [8], the equations for the correlations of the third-order pulsations of the dispersed-phase velocity were closed using the representations of the fourth moments involved in the indicated equations in the form of the sum of products of the second moments.

In the present work, a mathematical model has been developed for calculating a rising gas-dispersion flow in the stabilized region of a tube on the basis of the so-called two-fluid models in which a gas and a solid phase are considered as mutually penetrating continuous media. This model includes equations for determining the second, third, and fourth moments of the pulsation velocities of the particles with account for the interphase and interparticle inter-

Institute of Coal Power Production, National Academy of Sciences and Mintopenergo of Ukraine, 19 Andreevskaya Str., Kiev, 04070, Ukraine. Translated from Inzhenerno-Fizicheskii Zhurnal, Vol. 80, No. 4, pp. 99–109, July–August, 2007. Original article submitted November 19, 2005.

1062-0125/07/8004-0742

actions. The equation of motion of the carrying medium is closed on the basis of the one-parameter model of turbulence extended to the case of two-phase turbulent flows [2]. In [9, 10], the equations of transfer of the correlations of the pulsation velocities of the particles in the region of steady motion of the dispersed phase were constructed by a special computational technique that includes two variants of closing of the equations for the third moments; these variants differ by the method of determining the fourth correlations involved in the equations. In the first variant, the indicated equations are closed using the Millionshchikov hypothesis, in accordance with which the fourth-order cumulants are equal to zero and the fourth moments represent the sum of products of the second moments. This approach makes it possible to obtain, using the equations for the third moments, algebraic relations for the third-order correlations expressed in terms of the second moments and their gradients. In the second variant, the fourth-order correlations are determined from the equations of transfer of the correlations themselves. In this case, the fifth moments involved in these equations represent the sums of products of the second- and third-order correlations. This makes it possible to obtain, using the equations for the fourth moments, algebraic relations for the fourth moments expressed in terms of the second and third correlations and their derivatives. In the present work, we consider the case where the equations for the variables $\langle v'_p v'_p v'_p \rangle$, $\langle v'_p w'_p w'_p \rangle$, $\langle v'_p v'_p w'_p \rangle$, $\langle w'_p w'_p w'_p \rangle$, $\langle u'_p u'_p v'_p \rangle$, and $\langle w'_p v'_p u'_p \rangle$ are closed by the first variant (see Eqs. (30), (33)–(37) in [9]) and the equations for $\langle u'_p w'_p w'_p \rangle$ and $\langle u'_p v'_p v'_p \rangle$ are closed in accordance with the second variant (see Eqs. (9), (11) in [10]).

The system of equations defining the behavior of a two-phase turbulent flow in the stabilized section of a round tube includes

the momentum-transfer equation for the carrying medium and the solid phase

$$\frac{\rho_g}{r}\frac{\partial}{\partial r}\left[r\,(\eta_{t,g}+\eta_g)\frac{\partial u_g}{\partial r}\right]-\frac{\partial P}{\partial z}-F_{az}=0\,,\quad \frac{\rho_p\beta}{r}\frac{\partial}{\partial r}\left(r\,\langle u'_p v'_p\rangle\right)-F_{az}+\rho_p\beta g=0 \tag{1}$$

and the equation of transfer of the gas turbulent energy

$$\frac{\rho_g}{r}\frac{\partial}{\partial r}\left[r\left(\frac{\eta_{t,g}}{\sigma_k}+\eta_g\right)\frac{\partial k_g}{\partial r}\right]+\rho_g\eta_{t,g}\left(\frac{\partial u_g}{\partial r}\right)^2-\rho_g\,(\varepsilon_g+\varepsilon_p)+G=0\,. \tag{2}$$

Unlike [11], where the double correlation $\langle u'_p v'_p\rangle$ involved in the averaged equation of particle motion was calculated using the gradient representations $\langle u'_p v'_p\rangle = -\eta_{t,p}\partial u_p/\partial r$, we determined this variable from the equation of its transfer [10]:

$$\begin{aligned}
\rho_p\beta\Bigg[&\frac{2\partial}{3r\partial r}\left(r\tau\,\langle v'^2_p\rangle\,\frac{\partial\,\langle u'_p v'_p\rangle}{\partial r}\right)-\frac{\partial}{3r\partial r}\left(r\tau\,\langle u'_p v'_p\rangle\,\frac{\partial\,\langle v'^2_p\rangle}{\partial r}\right)-\frac{\partial}{3r\partial r}\left(r\tau\,\langle v'^3_p\rangle\,\frac{\partial u_p}{\partial r}\right)-\\
&-\frac{\partial}{6r\partial r}\left(\tau^2\,\langle v'^2_p\rangle\,\frac{\partial\,\langle u'_p w'^2_p\rangle}{\partial r}\right)-\frac{\partial}{6r\partial r}\left(\tau^2\,\langle u'_p v'_p\rangle\,\frac{\partial\,\langle v'_p w'^2_p\rangle}{\partial r}\right)-\\
&-\frac{\partial}{3r\partial r}\left(\tau^2\,\langle w'_p v'_p\rangle\,\frac{\partial\,\langle w'_p v'_p u'_p\rangle}{\partial r}\right)-\frac{\partial}{6r\partial r}\left(\tau^2\,\langle v'^2_p\rangle\,\langle w'^2_p\rangle\,\frac{\partial u_p}{\partial r}\right)-\\
&-\frac{\partial}{3r\partial r}\left(\tau^2\,\langle w'_p v'_p\rangle^2\,\frac{\partial u_p}{\partial r}\right)-\frac{\partial}{3r\partial r}\,\frac{(\tau^2\,\langle v'^2_p\rangle\,\langle u'_p w'^2_p\rangle)}{r}-\frac{\partial}{3r\partial r}\,\frac{(\tau^2\,\langle u'_p v'_p\rangle\,\langle v'_p w'^2_p\rangle)}{r}-\\
&-\frac{\partial}{3r\partial r}\,\frac{(\tau^2\,\langle w'_p v'_p u'_p\rangle\,\langle w'_p v'_p\rangle)}{r}+\frac{\partial}{3r\partial r}\,\frac{(\tau^2\,\langle w'^2_p\rangle\,\langle u'_p w'^2_p\rangle)}{r}+\frac{\partial}{6r\partial r}\,\frac{(\tau^2\,\langle u'_p w'_p\rangle\,\langle w'^3_p\rangle)}{r}-\\
&-\frac{2\partial\,(\tau\,\langle w'_p w'_p\rangle\,\langle u'_p v'_p\rangle)}{3r\partial r}+\frac{\langle v'_p v'_p\rangle\,\partial u_p}{\partial r}-\frac{\langle u'_p w'_p w'_p\rangle}{r}\Bigg]=
\end{aligned} \tag{3}$$

$$= \frac{\rho_p \beta}{\tau}\left(\langle u_p' v_g' \rangle + \langle u_g' v_p' \rangle - 2\langle u_p' v_p' \rangle\right).$$

The system of equations (1)–(3) is nonclosed because Eq. (3) involves the unknown second-order correlations $\langle v_p'^2 \rangle$, $\langle w_p' v_p' \rangle$, $\langle w_p'^2 \rangle$, and $\langle u_p' w_p' \rangle$, third-order correlations $\langle v_p'^3 \rangle$, $\langle u_p' w_p'^2 \rangle$, $\langle v_p' w_p'^2 \rangle$, $\langle w_p' v_p' u_p' \rangle$, and $\langle w_p'^3 \rangle$, and the product moments $\langle u_p' v_g' \rangle$ and $\langle u_g' v_p' \rangle$. These product moments are determined in accordance with the recommendations proposed in [2], and the correlations related to the dispersed phase are determined from the system of equations (30), (34)–(37), (39)–(41), proposed in [9], and from Eqs. (9) and (11) with boundary conditions (13)–(15), (18), and (19), proposed in [10]. Some of these equations we will use in the further numerical analysis. They are

the equation of transfer of the quantity $\langle v_p' v_p' \rangle$

$$\rho_p \beta\left[\frac{\partial}{r\partial r}\left(r\tau\langle v_p' v_p' \rangle \frac{\partial \langle v_p' v_p' \rangle}{\partial r}\right) - \frac{2}{r}\frac{\partial\left(\tau\langle w_p' v_p' \rangle^2\right)}{\partial r} - \frac{2\tau\langle v_p' v_p' \rangle}{3r}\frac{\partial \langle w_p' w_p' \rangle}{\partial r} - \right.$$

$$\left. - \frac{4\tau\langle w_p' v_p' \rangle}{3r}\frac{\partial \langle w_p' v_p' \rangle}{\partial r} + \frac{4\tau\langle w_p' w_p' \rangle^2}{3r^2} - \frac{4\tau\langle v_p' v_p' \rangle\langle w_p' w_p' \rangle}{3r^2} - \frac{4\tau\langle w_p' v_p' \rangle^2}{3r^2}\right] + \frac{2\rho_p \beta}{\tau} \times \tag{4}$$

$$\times\left(\langle v_p' v_g' \rangle - \langle v_p' v_p' \rangle\right) + 2\left\{\frac{\delta^2 \rho_p}{6912\beta}\left(\frac{\partial u_p}{\partial r}\right)^2\left(\frac{1-K_n}{2} - \frac{1-K_\tau}{7}\right)^2 - C_1 \rho_p \beta \langle v_p' v_p' \rangle (1-K_n^2)\right\} N = 0;$$

the equation of transfer of the quantity $\langle w_p' v_p' \rangle$

$$\rho_p \beta\left[\frac{2\partial}{3r\partial r}\left(r\tau\langle v_p' v_p' \rangle \frac{\partial \langle w_p' v_p' \rangle}{\partial r}\right) + \frac{2}{3r}\frac{\partial\left(\tau\langle v_p' v_p' \rangle \langle w_p' v_p' \rangle\right)}{\partial r} + \right.$$

$$+ \frac{\partial}{3r\partial r}\left(r\tau\langle w_p' v_p' \rangle \frac{\partial \langle v_p' v_p' \rangle}{\partial r}\right) - \frac{4}{3r}\frac{\partial\left(\tau\langle w_p' v_p' \rangle \langle w_p'^2 \rangle\right)}{\partial r} - \frac{\tau\langle w_p' v_p' \rangle}{r}\frac{\partial \langle w_p' w_p' \rangle}{\partial r} -$$

$$- \frac{10\tau\langle w_p' v_p' \rangle \langle w_p' w_p' \rangle}{3r^2} + \frac{2\tau\langle v_p' v_p' \rangle}{3r}\frac{\partial \langle w_p' v_p' \rangle}{\partial r} + \frac{2\tau\langle v_p' v_p' \rangle \langle w_p' v_p' \rangle}{3r^2} + \tag{5}$$

$$\left. + \frac{\tau\langle w_p' v_p' \rangle}{3r}\frac{\partial \langle v_p' v_p' \rangle}{\partial r}\right] + \frac{\rho_p \beta}{\tau}\left(\langle v_g' w_p' \rangle + \langle v_p' w_g' \rangle - 2\langle w_p' v_p' \rangle\right) = 0;$$

the equation of transfer of the quantity $\langle u_p' u_p' \rangle$

$$\rho_p \beta\left[-\frac{\partial}{6r\partial r}\left(r\tau\langle v_p' v_p' \rangle \frac{\partial \langle u_p' u_p' \rangle}{\partial r}\right) - \frac{\partial}{3r\partial r}\left(r\tau\langle u_p' v_p' \rangle \frac{\partial \langle u_p' v_p' \rangle}{\partial r}\right) - \right.$$

$$\left. - \frac{\partial}{3r\partial r}\left(r\tau\langle u_p' v_p'^2 \rangle \frac{\partial u_p}{\partial r}\right) + \frac{\partial\left(\tau\langle u_p' w_p' \rangle^2\right)}{3r\partial r} + \langle u_p' v_p' \rangle \frac{\partial u_p}{\partial r}\right] = \frac{\rho_p \beta}{\tau}\left(\langle u_p' u_g' \rangle - \langle u_p' u_p' \rangle\right) + \tag{6}$$

$$+ \left\{\frac{\delta^2 \rho_p}{576\beta}\left(\frac{\partial u_p}{\partial r}\right)^2\left[\frac{(1-K_n)(1-K_\tau)}{14} + \frac{1}{3}\left(\frac{1-K_n}{2} - \frac{1-K_\tau}{7}\right)^2\right] - C_3 \rho_p \beta \langle u_p' u_p' \rangle (1-K_n^2)\right\} N, \quad K_n < 0;$$

the algebraic expression for the correlation $\langle u'_p u'_p v'_p \rangle$

$$\langle u'_p u'_p v'_p \rangle = -\tau \left[\frac{2 \langle u'_p v'_p \rangle \partial \langle u'_p v'_p \rangle}{3\partial r} + \frac{\langle v'_p v'_p \rangle \partial \langle u'_p u'_p \rangle}{3\partial r} + \frac{2 \langle u'_p v'_p v'_p \rangle \partial u_p}{3\partial r} - \frac{2 \langle u'_p w'_p \rangle^2}{3r} \right]; \quad (7)$$

the algebraic expression for the quantity $\langle u'_p v'_p v'_p \rangle$

$$\langle u'_p v'_p v'_p \rangle = -\tau \left[\frac{\langle u'_p v'_p \rangle \partial \langle v'_p v'_p \rangle}{3\partial r} + \frac{2 \langle v'_p v'_p \rangle \partial \langle u'_p v'_p \rangle}{3\partial r} + \frac{\langle v'_p v'_p v'_p \rangle \partial u_p}{3\partial r} + \right.$$

$$+ \frac{\tau \langle v'_p v'_p \rangle \partial \langle u'_p w'_p w'_p \rangle}{6r\partial r} + \frac{\tau \langle u'_p v'_p \rangle \partial \langle v'_p w'_p w'_p \rangle}{6r\partial r} + \frac{\tau \langle w'_p v'_p \rangle \partial \langle w'_p v'_p u'_p \rangle}{3r\partial r} +$$

$$+ \frac{\tau \langle v'_p v'_p \rangle \langle w'_p w'_p \rangle \partial u_p}{6r\partial r} + \frac{\tau \langle w'_p v'_p \rangle^2 \partial u_p}{3r\partial r} + \frac{\tau \langle v'_p v'_p \rangle \langle u'_p w'_p w'_p \rangle}{3r^2} + \frac{\tau \langle u'_p v'_p \rangle \langle v'_p w'_p w'_p \rangle}{3r^2} +$$

$$\left. + \frac{\tau \langle w'_p v'_p u'_p \rangle \langle w'_p v'_p \rangle}{3r^2} - \frac{\tau \langle w'_p w'_p \rangle \langle u'_p w'_p w'_p \rangle}{3r^2} - \frac{\tau \langle u'_p w'_p \rangle \langle w'^3_p \rangle}{6r^2} + \frac{2 \langle w'_p w'_p \rangle \langle u'_p v'_p \rangle}{3r} \right]; \quad (8)$$

and the algebraic expression for the third moment of the pulsations of the radial velocity of the particles

$$\langle v'_p v'_p v'_p \rangle = -\tau \left[\langle v'_p v'_p \rangle \frac{\partial \langle v'_p v'_p \rangle}{\partial r} - \frac{2 \langle w'_p v'_p \rangle^2}{r} \right]. \quad (9)$$

This system of equations was integrated by the method of marching with iterations on a nonuniform grid bunched near the wall of the channel; in this case, the pressure gradient was eliminated by the known method described in [12]. On the basis of the algorithm described, we have developed a program that was used for numerical investigation of the main mechanisms of the rising gas-suspension flow.

We will consider four computational variants in which different mean velocities of the carrying medium (averaged over the cross section of the tube) $u_{g,m}$ and different particle sizes δ are used: I) $u_{g,m}$ = 8 m/sec, $\delta = 0.2 \cdot 10^{-3}$ m; II) $u_{g,m}$ = 10 m/sec, $\delta = 0.1 \cdot 10^{-3}$ m; III) $u_{g,m}$ = 15 m/sec, $\delta = 0.05 \cdot 10^{-3}$ m; IV) $u_{g,m}$ = 6.5 m/sec, $\delta = 0.28 \cdot 10^{-3}$ m. In all the variants, β = 0.0012, ρ_g = 1.3 kg/m^3, and ρ_p = 1600 kg/m^3. Figures 1–10 illustrate the features of the aerodynamics of a two-phase flow in a channel of radius R = 0.1 m. In Fig. 1, the calculated values of the longitudinal velocities of the carrying medium and the solid phase in the stabilized region of a two-phase flow are presented. It is seen from this figure that, in the central region of the channel, a decrease in the particle size from $0.28 \cdot 10^{-3}$ m to $0.05 \cdot 10^{-3}$ m leads to a significant decrease in the velocity of the interphase sliding $u_g(r) - u_p(r)$ (curves 5 and 6 and 7 and 8 are compared). At the wall of the channel, where the velocity of the carrying medium tends to zero, the particles move more rapidly than the gas because of the action of the shear Reynolds stress $\langle u'_p v'_p \rangle$ (see (1), the first term of the second equation). Such behavior of the functions $u_g(r)$ and $u_p(r)$ in the near-wall region is qualitatively consistent with the experimental data [13] obtained for the stabilized section of a tube with a radius R = 0.015 m.

Figure 2 shows the distribution of the kinetic pulsation energy of the carrying medium in the region of steady motion of the gas suspension. It is seen from this figure that, in the near-axis region $0 < r <$ 0.018 m, the turbulent energy of the gas in variant IV is somewhat higher than that in variants I–III. This is explained by the fact that the generation of the pulsation gas energy in the wakes after the particles G (see (2)) increases with increase in the diameter of the dispersed phase. In the interval 0.018 m $< r <$ 0.096 m, the rate of generation of the turbulent gas energy in the process of transformation of the averaged-motion energy into the energy of pulsations (the second term in Eq. (2)) is higher in variant III than in the other variants $((\partial u_g/\partial r)_{III} > (\partial u_g/\partial r)_s$, s = I, II, IV); therefore, the values of the function $k_g(r)$ in variant III are somewhat larger than those in variants I, II, and IV.

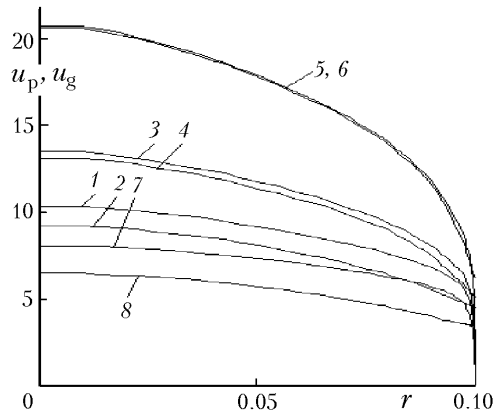

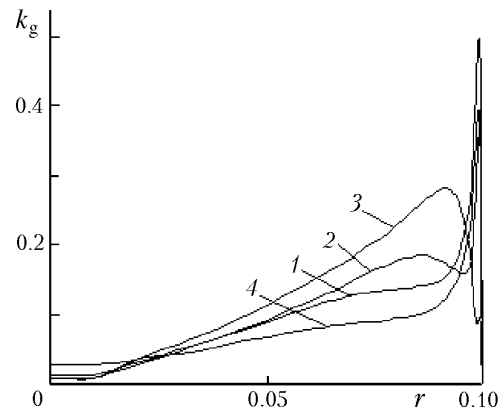

Fig. 1. Profiles of the averaged axial velocities of the gas and the particles: variant I: 1) u_g, 2) u_p; II: 3) u_g, 4) u_p; III: 5) u_g, 6) u_p; IV: 7) u_g, 8) u_p.

Fig. 2. Profiles of the kinetic energy of the turbulent gas-velocity pulsations k_g: variant I (1), II (2), III (3), and IV (4).

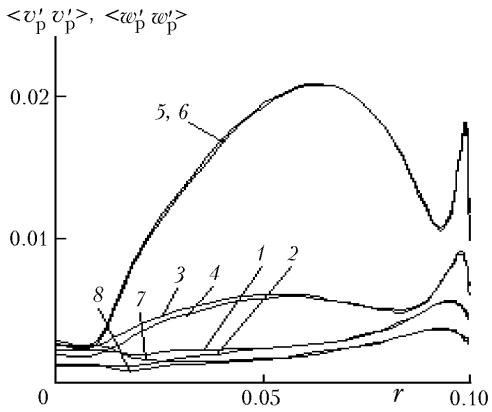

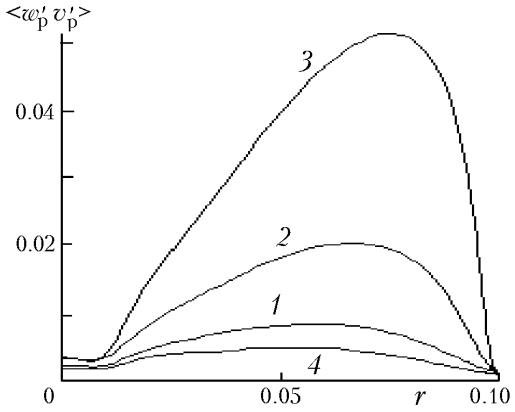

Fig. 3. Profiles of the second correlation moments of the dispersed-phase velocity pulsations: variant I: 1) $\langle w'_p w'_p \rangle$, 2) $\langle v'_p v'_p \rangle$; II: 3) $\langle w'_p w'_p \rangle$, 4) $\langle v'_p v'_p \rangle$; III: 5) $\langle w'_p w'_p \rangle$, 6) $\langle v'_p v'_p \rangle$; IV: 7) $\langle w'_p w'_p \rangle$, 8) $\langle v'_p v'_p \rangle$.

Fig. 4. Distribution of the shear Reynolds stress $\langle w'_p v'_p \rangle$ over the cross section of the flow: variant I (1), II (2), III (3), IV (4).

Figure 3 shows the distribution of the components of the chaotic-motion energy of the particles $\langle w'_p w'_p \rangle$ and $\langle v'_p v'_p \rangle$ over the cross section of the flow. Analysis of the numerical results shows that the behavior of the function $\langle v'_p v'_p \rangle(r)$ (curve 6) depends mainly on the rate of generation of the particle pulsation energy (turbulent and pseudoturbulent) in the process of the interphase and interparticle interactions. In the region $0.0095 < r < 0.0668$ m, the character of the dependence $\langle v'_p v'_p \rangle(r)$ is determined by the rate of generation of the turbulent dispersed-phase energy that increases with increase in the function $\langle v'_p v'_g \rangle$ (eighth term in Eq. (4)). In the region $0.0668 < r < 0.094$ m, the decrease in the dependence $\langle v'_p v'_p \rangle(r)$ is caused by the large decrease in the value of $\langle v'_p v'_g \rangle$. In the region $0.094 < r < 0.0993$ m, the rate of generation of the pseudoturbulent energy of the particles (the tenth term in Eq. (4)) significantly exceeds the rate of generation of the turbulent pulsation energy of the particles because of the large increase in the value of $|\partial u_p / \partial r|$ (Fig. 1, curve 6). Therefore, the dependence $\langle v'_p v'_p \rangle(r)$ increases sharply in this region. Near the wall of the channel, where $r > 0.0993$ m, the function $\langle v'_p v'_p \rangle(r)$ decreases as a result of the decrease in the rate of generation of the pulsation energy of the particles.

It follows from the figure that the character of change in the curves $\langle w'_p w'_p \rangle(r)$ is close to the character of change in the curves $\langle v'_p v'_p \rangle(r)$; in this case, the values of the functions $\langle w'_p w'_p \rangle(r)$ and $\langle v'_p v'_p \rangle(r)$ for particles of small

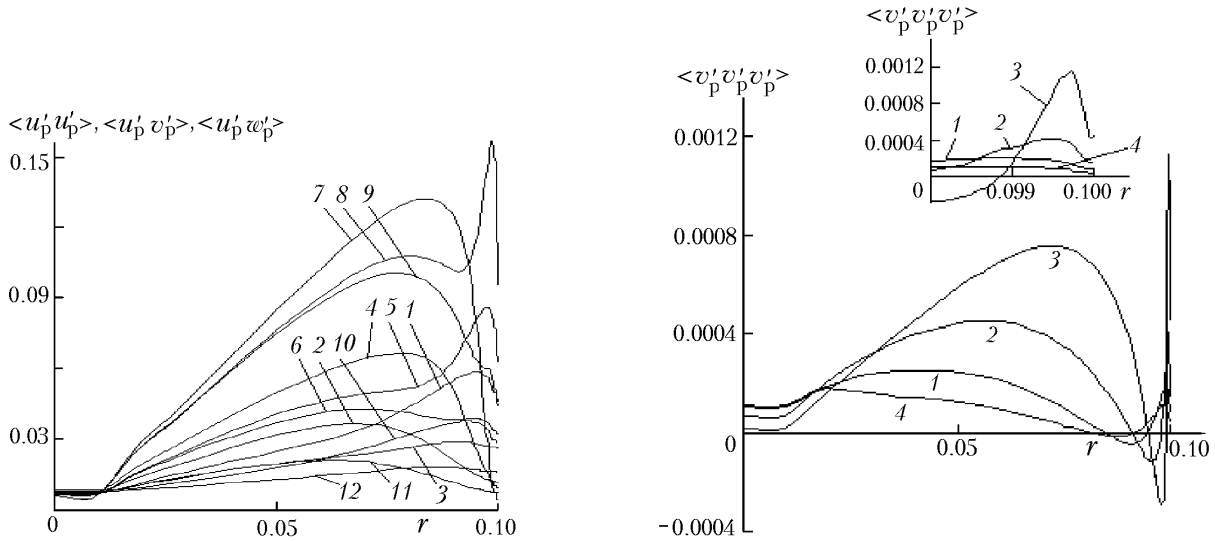

Fig. 5. Distribution of the second moments of the particle-velocity pulsations over the cross section of the flow: variant I: 1) $\langle u'_p u'_p \rangle$, 2) $\langle u'_p w'_p \rangle$, 3) $\langle u'_p v'_p \rangle$; variant II: 4) $\langle u'_p w'_p \rangle$, 5) $\langle u'_p u'_p \rangle$, 6) $\langle u'_p v'_p \rangle$; variant III: 7) $\langle u'_p w'_p \rangle$, 8) $\langle u'_p u'_p \rangle$, 9) $\langle u'_p v'_p \rangle$; variant IV: 10) $\langle u'_p u'_p \rangle$, 11) $\langle u'_p w'_p \rangle$, 12) $\langle u'_p v'_p \rangle$.

Fig. 6. Distribution of the third moment of pulsations of the dispersed-phase radial velocity $\langle v'_p v'_p v'_p \rangle$ over the cross section of the flow: variant I (1), II (2), III (3), and IV (4).

sizes are practically equal (curves 5, 6) and these functions for large particles are somewhat different (cf. curves 1 and 2, 3 and 4, and 7 and 8).

Figure 4 presents results of calculations of the shear Reynolds stress $\langle w'_p v'_p \rangle$ in the region of steady motion of the gas suspension. It is seen from this figure that the function $\langle w'_p v'_p \rangle(r)$ has a maximum at the point r = 0.076 m (curve 3). In the region $0.0095 < r < 0.076$ m, this curve grows steeply, which is explained by the increase in the rate of generation of the Reynolds stress $\langle w'_p v'_p \rangle$ under the action of the aerodynamic drag (the tenth and eleventh terms in Eq. (5) $\rho_p \beta(\langle v'_g w'_p \rangle + \langle v'_p w'_g \rangle)/\tau$). In the region corresponding to the descending branch of the curve, the rate of generation of the shear Reynolds energy decreases substantially due to the decrease in the functions $\langle v'_g w'_p \rangle(r)$ and $\langle v'_p w'_g \rangle(r)$ in this region; as a result, the derivative $\partial \langle w'_p v'_p \rangle / \partial r$ becomes negative.

Figure 5 shows the distribution of the shear and normal Reynolds stresses over the cross section of the flow. Analysis of the balance of the terms of Eq. (6) shows that the main contribution to the formation of the profile $\langle u'_p u'_p \rangle(r)$ (curve 8) is made by the fifth, sixth, and eighth terms of the indicated equation. In the region $0.0095 < r < 0.08$ m, where the influence of the interparticle collisions on the character of the curve $\langle u'_p u'_p \rangle(r)$ is small (the eighth term of the equation), the rapid growth of the dependence $\langle u'_p u'_p \rangle(r)$ is due to the sharp increase in the functions $\langle u'_p v'_p \rangle(r)$ (Fig. 5, curve 9) and $\langle u'_p u'_g \rangle(r)$ in this region. In the region $0.08 < r < 0.092$ m, the rate of generation of the turbulent energy of the particles (the sixth term in the equation) decreases as a result of the decrease in the value of $\langle u'_p u'_g \rangle$, which leads to some decay of the curve $\langle u'_p u'_p \rangle(r)$. In the region $0.092 < r < 0.099$ m, the rate of generation of the kinetic pulsation energy of the particles in the process of transformation of the averaged-motion energy into the energy of pulsations (the fifth term in the equation) and the interparticle interactions increases because of the large increase in the modulus of the gradient of the axial velocity of the particles $|\partial u_p / \partial r|$. Therefore, the function $\langle u'_p u'_p \rangle(r)$ increases sharply in this region. Near the wall of the channel the rate of generation of the chaotic-motion energy of the dispersed phase decreases markedly, which leads to a decay of the curve $\langle u'_p u'_p \rangle(r)$.

It is seen from this figure that the behavior of the curve $\langle u'_p v'_p \rangle(r)$ in the region $0.095 < r < 0.078$ m is similar in character to the dependence $\langle u'_p u'_p \rangle(r)$ in this zone (cf. curves 8 and 9). The sharp increase in the function $\langle u'_p v'_p \rangle(r)$ in this region is due to the increase in the fifteenth $\rho_p \beta \langle v'_p v'_p \rangle / \partial u_p / \partial r$, seventeenth $\rho_p \beta \langle u'_p v'_g \rangle / \tau$, and eighteenth $\rho_p \beta \langle u'_g v'_p \rangle / \tau$ terms of Eq. (3). In the peripheral region, on the one hand, the mixed correlation moments

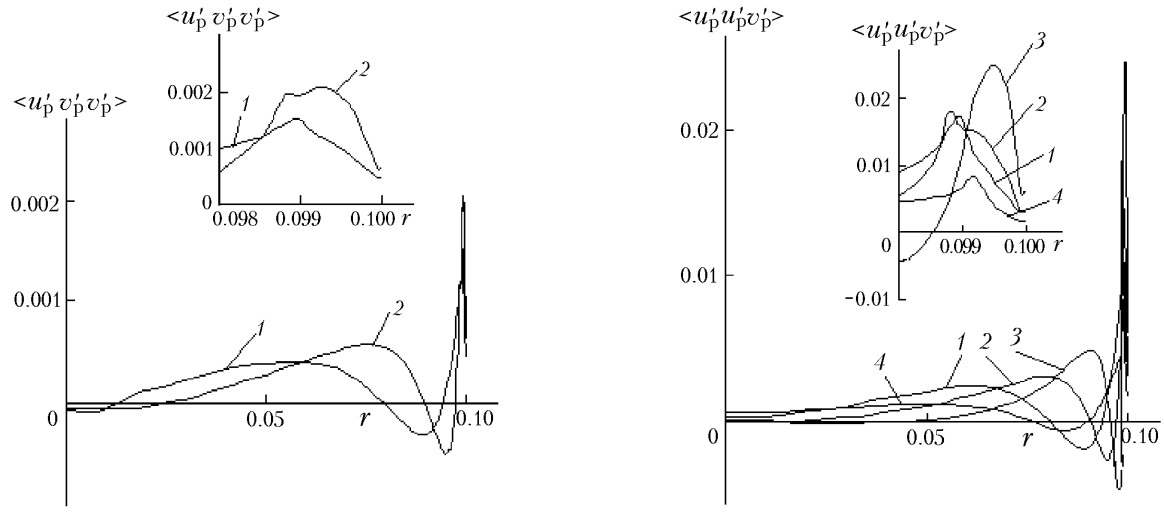

Fig. 7. Distribution of the third-order correlations $\langle u'_p v'_p v'_p \rangle$ over the region of steady motion of a two-phase flow: variant I (1), II (2).

Fig. 8. Distribution of the third correlation moment $\langle u'_p u'_p v'_p \rangle$ over the cross section of the flow: variant I (1), II (2), III (3), and IV (4).

$\langle u'_p v'_g \rangle$ and $\langle u'_g v'_p \rangle$ are substantially decreased, and on the other the rate of generation of the shear Reynolds stress $\langle u'_p v'_p \rangle$ in the process of mutual transformations of the averaged-motion and chaotic-motions energies of the solid phase (the fifteenth term of the equation) is increased, which leads to a decay of the curve $\langle u'_p v'_p \rangle(r)$ in this region.

When the dependences of the components of the particle pulsation energy (curves 5 and 6 in Fig. 3 and curve 8 in Fig. 5) are compared, it is apparent that the curve $\langle u'_p u'_p \rangle(r)$ is similar to the curves $\langle w'_p w'_p \rangle(r)$ and $\langle v'_p v'_p \rangle(r)$. In this case, the values of the function $\langle u'_p u'_p \rangle(r)$ are much larger than the values of $\langle w'_p w'_p \rangle(r)$ and $\langle v'_p v'_p \rangle(r)$. For example, the ratio $\langle u'_p u'_p \rangle / \langle w'_p w'_p \rangle$ is equal to 2.8 at the axis of the flow and 8.3 near the wall (r = 0.099 m), which points to the fact that the field of the solid-phase pulsation energy is anisotropic.

In Fig. 6, the values of the third moment of the radial-velocity pulsations of the particles $\langle v'_p v'_p v'_p \rangle$ in the region of stabilized gas-suspension flow are presented. The results of the calculations show that the second term in Eq. (9) $2\tau \langle w'_p v'_p \rangle^2 / r$ is the main factor determining the increase in the dependence $\langle v'_p v'_p v'_p \rangle(r)$ (curve 3) in the region $0.0095 < r < 0.075$ m. In the region $0.075 < r < 0.095$ m, the dependence $\langle v'_p v'_p v'_p \rangle(r)$ decreases due to the decrease in the shear Reynolds stress $\langle w'_p v'_p \rangle$ and the increase in the radial coordinate r (curve 3 in Fig. 4). In the region $0.095 < r < 0.098$ m, corresponding to the decaying branch of the curve $\langle v'_p v'_p v'_p \rangle(r)$, the behavior of this curve depends substantially on the first term of the indicated equation, which is explained by the increase in the dependence $\langle v'_p v'_p \rangle(r)$ and in its derivative (curve 6 in Fig. 3). In the region $0.098 < r < 0.099$ m, where the derivative $\partial \langle v'_p v'_p \rangle / \partial r$ tends to zero, the function $\langle v'_p v'_p v'_p \rangle(r)$ increases as a result of the decrease in the first term of the equation. The further increase in the curve $\langle v'_p v'_p v'_p \rangle(r)$ in the region $0.099 < r < 0.0996$ m is due to the change in the sign of the derivative ($\partial \langle v'_p v'_p \rangle / \partial r < 0$) and the increase in its absolute value. In the near-wall region where $r > 0.0996$ m, the dependence $\langle v'_p v'_p v'_p \rangle(r)$ decreases sharply, which is explained by the large decrease in the value of the second moment $\langle v'_p v'_p \rangle$.

Figure 7 shows the distribution of the third moment of the particle-velocity pulsations $\langle u'_p v'_p v'_p \rangle$ over the cross section of the flow. In the region $0.018 < r < 0.06$ m, corresponding to the rising branch of the curve $\langle u'_p v'_p v'_p \rangle(r)$ (curve 1), the behavior of this curve is determined by the third and eighth terms of Eq. (8). Here, the function $\langle u'_p v'_p v'_p \rangle(r)$ increases monotonically due to the growth of the curves $\langle v'_p v'_p v'_p \rangle(r)$ and $\langle w'_p v'_p \rangle(r)$ and the increase in the absolute value of the axial-velocity of the particles $\left| \partial u_p / \partial r \right|$ in this region (curve 2 in Fig. 1, curve 1 in Fig. 4, curve 1 in Fig. 6). In the region $0.06 < r < 0.09$ m, corresponding to the decaying branch of the curve $\langle u'_p v'_p v'_p \rangle(r)$, the behavior of this curve is determined by the first, third, seventh, eighth, and fourteenth terms of the indicated equation. The function $\langle u'_p v'_p v'_p \rangle(r)$ decreases in the region $0.06 < r < 0.08$ m, which is explained by the decay of the curves $\langle v'_p v'_p v'_p \rangle(r)$ and $\langle w'_p v'_p v'_p \rangle(r)$ and the increase in the dependences $\langle u'_p v'_p \rangle(r)$, $\langle v'_p v'_p \rangle(r)$, and $\langle w'_p w'_p \rangle(r)$ (curves 1 and 2 in Fig. 3, curve 3 in Fig. 5). When the coordinate r increases further ($0.08 < r < 0.09$ m), the function

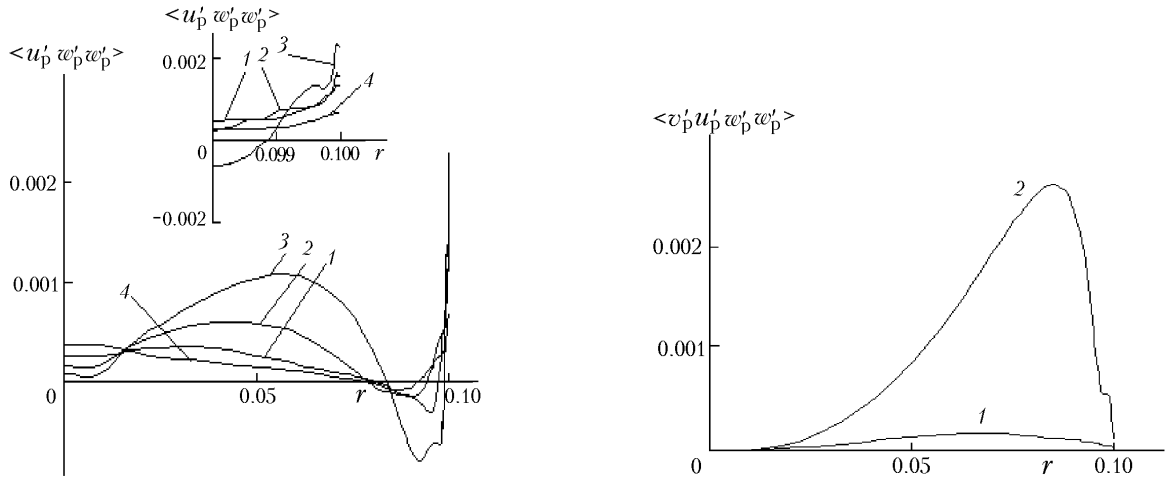

Fig. 9. Profiles of the third moment of the particle-velocity pulsations $\langle u'_p w'^2_p \rangle$: variant I (1), II (2), III (3), and IV (4).

Fig. 10. Profiles of the fourth moment of the particle-velocity pulsations $\langle v'_p u'_p w'^2_p \rangle$: variant I (1), III (2).

$\langle v'_p v'_p v'_p \rangle(r)$ becomes negative and its absolute value increases; therefore, the curve $\langle u'_p v'_p v'_p \rangle(r)$ continues to decay in this region. In the region $0.09 < r < 0.094$ m, where the function $\langle v'_p v'_p v'_p \rangle(r)$ and the gradient $\partial \langle v'_p v'_p \rangle / \partial r$ tends to zero, the growth of the curve $\langle u'_p v'_p v'_p \rangle(r)$ is determined by the second and fourteenth terms of the equation. In the near-wall zone $0.094 < r < 0.0994$ m, the dependence $\langle v'_p v'_p v'_p \rangle(r)$ increases rapidly and the ratio $\left| \partial \langle v'_p v'_p \rangle / \partial r \right|$ (the first and third terms of the equation) increases substantially, which provides a further growth of the curve $\langle u'_p v'_p v'_p \rangle(r)$.

In Fig. 8, the values of the third correlation moment $\langle u'_p u'_p v'_p \rangle$ in the region of steady motion of the two-phase flow are presented. As the calculation results show, the behavior of the curve $\langle u'_p u'_p v'_p \rangle(r)$ (curve 1) is determined by the rate of generation of the third moment $\langle u'_p u'_p v'_p \rangle$ in the process of transformation of the averaged-motion energy into the energy of pulsations $2\tau \langle u'_p u'_p v'_p \rangle \partial u_p / (3\partial r)$ (the third term of Eq. (7)) and by the value of $2\tau \langle u'_p w'_p \rangle^2 / (3r)$ (the fourth term of Eq. (7)). The curve $\langle u'_p u'_p v'_p \rangle(r)$ monotonically increases in the region $0 < r < 0.063$ m as a result of the increase in the correlation moments $\langle u'_p v'_p v'_p \rangle$ (curve 1 in Fig. 7) and $\langle u'_p w'_p \rangle$ (curve 2 in Fig. 5) and in the absolute value of the derivative of the particle axial velocity $\left| \partial u_p / \partial r \right|$ (curve 2 in Fig. 1). The dependence $\langle u'_p u'_p v'_p \rangle(r)$ decreases in the region $0.063 < r < 0.082$ m because of the decrease in the correlations $\langle u'_p v'_p v'_p \rangle$ and $\langle u'_p w'_p \rangle$ and the increase in the coordinate r in this region. In the region $0.082 < r < 0.09$ m, where the function $\langle u'_p v'_p v'_p \rangle(r)$ takes negative values, the third term of the equation begins to prevail substantially over the fourth term due to the increase in the absolute value of the third moment $\langle u'_p v'_p v'_p \rangle$; therefore, $\langle u'_p u'_p v'_p \rangle(r)$ continues to decrease in this zone. In the peripheral region, where $r > 0.09$ m, the change in the curve $\langle u'_p u'_p v'_p \rangle(r)$ is determined by the behavior of the dependence $\langle u'_p v'_p v'_p \rangle(r)$ in this region. For example, the sharp growth of the curve $\langle u'_p u'_p v'_p \rangle(r)$ in the region $0.09 < r < 0.099$ m is explained by the rapid increase in the dependence $\langle u'_p v'_p v'_p \rangle(r)$, and the decrease in the function $\langle u'_p u'_p v'_p \rangle(r)$ near the wall of the channel, where $r > 0.099$ m, is due to the decrease in the value of $\langle u'_p v'_p v'_p \rangle$.

Figure 9 presents the results of calculations of the third moment of the particle-velocity pulsations $\langle u'_p w'^2_p \rangle$. These data point to the fact that the function $\langle u'_p w'^2_p \rangle(r)$ increases when the velocity of the gas increases and the diameter of the solid phase decreases.

In Fig. 10, the distribution of the correlation $\langle v'_p u'_p w'^2_p \rangle$ over the cross section of the flow is shown. When the dependences $\langle u'_p w'^2_p \rangle(r)$ (curve 3 in Fig. 9) and $\langle v'_p u'_p w'^2_p \rangle(r)$ (curve 2 in Fig. 10) are compared, it is apparent that the values of the function $\langle u'_p w'^2_p \rangle(r)$ are higher than the values of $\langle v'_p u'_p w'^2_p \rangle(r)$ in the central region of the channel $0 < r < 0.055$ m and, in the peripheral region $0.055 < r < 0.098$ m, the value of $\langle v'_p u'_p w'^2_p \rangle$ substantially exceeds the value of $\langle u'_p w'^2_p \rangle$, which points to the necessity of taking into account the fourth correlations of the particle-velocity pulsations in calculating the aerodynamics of two-phase turbulent flows.

Thus, the mathematical model proposed allows one to correctly calculate the aerodynamic structure of a two-phase flow in the region of steady motion of a gas suspension. Our numerical investigations have shown that (1) the

behavior of monodisperse particles is determined, along with the turbulent transfer of the solid phase, by the pseudoturbulent effects arising as a result of the collisions between particles in the process of their averaged motion. The turbulent energy of the particle chaotic motion in the central part of the channel substantially exceeds the pseudoturbulent energy, and the pseudoturbulent energy is a determining factor in the peripheral zone where the turbulent energy is small; (2) the pulsation-energy components of the particles $\langle u'_p u'_p \rangle$, $\langle w'_p w'_p \rangle$, and $\langle v'_p v'_p \rangle$ are substantially different, which points to the fact that the field of the solid-phase pulsation energy is anisotropic; (3) the fourth moments of the particle pulsation velocities can influence the behavior of the dispersed phase more strongly that the third moments, which should be taken into account in calculating such systems.

NOTATION

C_1, C_3, empirical constants; F, force, kg/(sec^2·m^2); G, generation of the turbulent gas energy in the wakes after the particles, kg/(sec^3·m); g, free fall acceleration, m/sec^2; K, coefficient of velocity recovery in the process of an impact; k, kinetic pulsation energy, m^2/sec^2; N, frequency of impacts, 1/sec; P, gas pressure, N/m^2; R, radius of the channel, m; r and z, radial and longitudinal coordinates, m; u, v, w, averaged components of the velocity vector, m/sec; β, true volume concentration of particles; δ, diameter of a particle, m; ε, dissipation of the pulsation energy, m^2/sec^3; η, kinematic viscosity, m^2/sec; ρ, density, kg/m^3; σ, empirical constant; τ, time of the dynamic relaxation of a particle, sec. Subscripts: a, aerodynamic drag of a particle; g, gas; k, kinematic pulsation energy of the gas; m, mean velocity of the gas (averaged over the cross section of the tube); n, normal; p, particle; t, turbulent pulsations; τ, tangential; $'$, pulsation component in the time averaging; $\langle\ \rangle$, time averaging.

REFERENCES

1. R. I. Nigmatulin, *Principles of the Mechanics of Heterogeneous Media* [in Russian], Nauka, Moscow (1978).
2. A. A. Shraiber, L. B. Gavin, V. A. Naumov, and V. P Yatsenko, *Turbulent Gas-Suspension Flows* [in Russian], Naukova Dumka, Kiev (1978).
3. G. N. Abramovich, On the influence of an admixture of solid particles or drops on the structure of a turbulent gas jet, *Dokl. Akad. Nauk SSSR*, **190**, No. 5, 1052–1055 (1970).
4. Yu. V. Zuev and I. A. Lepeshinskii, A mathematical model of a two-phase turbulent jet, *Izv. Akad. Nauk SSSR, Mekh. Zhidk. Gaza*, No. 6, 69–77 (1981).
5. D. Miloevich, O. P. Solonenko, and G. M. Krylov, A comparative analysis of some models of turbulent transfer of inertial particles, in: *Transfer Processes in Single- and Two-Phase Media* [in Russian], Inst. Teplofiziki, SO AN SSSR, Novosibirsk (1986), pp. 70–80.
6. L. V. Kondrat'ev, *A Model and Numerical Investigation of a Turbulent Gas-Suspension Flow in a Tube*, Authors's Abstract of Candidate's Dissertation (in Physics and Mathematics), Leningrad (1989).
7. I. V. Derevich and V. M. Eroshenko, Calculation of the averaged velocity slip of phases in turbulent dispersed flows in channels, *Izv. Akad. Nauk SSSR, Mekh. Zhidk. Gaza*, No. 2, 69–78 (1990).
8. L. I. Zaichik, Equations for the probability density function of the velocity of particles in an inhomogeneous turbulent field, *Izv. Akad. Nauk SSSR, Mekh. Zhidk. Gaza*, No. 2, 117–124 (1996).
9. B. B. Rokhman, Equations of transfer of the velocity pulsation correlation moments of the dispersed phase in the stabilized region of an axisymmetric two-phase flow. I. Equations for the second moments. Algebraic relations for the third correlations, *Prom. Teplotekh.*, **27**, No. 3, 9–16 (2005).
10. B. B. Rokhman, Equations of transfer of the velocity pulsation correlation moments of the dispersed phase in the stabilized region of an axisymmetric two-phase flow. II. Equations for the third correlation moments. Numerical results, *Prom. Teplotekh.*, **27**, No. 4, 27–35 (2005).
11. B. B. Rokhman, Calculation of the turbulent momentum transfer in a solid phase on the basis of equations for the second and third moments of the particle-velocity pulsations, *Inzh.-Fiz. Zh.*, **80**, No. 2, 60–70 (2007).
12. L. M. Simuni, Numerical solution of problems on the nonisothermal motion of a viscous liquid in a two-dimensional tube, *Inzh.-Fiz. Zh.*, **10**, No. 1, 86–91 (1966).
13. Y. Tsuji, Y. Morikawa, and H. Shiomi, LDV measurements of an air–solid two-phase flow in a vertical pipe, *Fluid Mech.*, **139**, 417–434 (1984).